Tetrahedron 66 (2010) 2501–2513

Contents lists available at ScienceDirect

Tetrahedron

journal homepage: www.elsevier.com/locate/tet

The interactions of bis-phenanthridinium–nucleobase conjugates with nucleotides: adenine-conjugate recognizes UMP in aqueous medium

Lidija-Marija Tumir [a], Marina Grabar [b], Sanja Tomić [b,*], Ivo Piantanida [a,*]

[a] Division of Organic Chemistry & Biochemistry, Ruđer Bošković Institute, HR 10002 Zagreb, P.O.B. 180, Croatia
[b] Laboratory for Chemical and Biological Crystallography, Division of Physical Chemistry, Ruđer Bošković Institute, HR 10002 Zagreb, P.O.B. 180, Croatia

ARTICLE INFO

Article history:
Received 14 August 2009
Received in revised form 9 December 2009
Accepted 18 January 2010
Available online 2 February 2010

ABSTRACT

Among series of novel bis-phenanthridinium–nucleobase conjugates, the adenine derivative revealed high (log Ks=6.9 M^{-1}) and selective affinity toward complementary nucleotide (UMP), accompanied by specific change in the UV–vis spectrum of phenanthridine subunits, differing significantly from changes caused by addition of other nucleotides. High stability and selectivity of adenine-conjugate/UMP non-covalent complex is, according to the molecular modeling studies, correlated to the number of inter- and intramolecular aromatic stacking interactions between phenanthridinium subunits, covalently attached adenine and added UMP, while the selectivity of adenine-conjugate toward UMP in respect to other nucleotides is most likely the consequence of additional hydrogen bonding between UMP and adenine.

1. Introduction

Efficient synthetic receptors with the capability of selective substrate binding in aqueous solution are important for the understanding of molecular recognition and self-assembly in chemical and biological systems.[1] Detection of nucleosides and nucleotides in aqueous medium has paramount importance as they form the fundamental units of all the life forms. However, differentiation among naturally occurring nucleobases based on different hydrogen bonding patterns within the artificial receptor is strongly limited due to competitive hydrogen bonding of water;[2] therefore among many artificial receptors reported, most of them lacked base selectivity. Actually, till now there are only a few receptors able to selectively bind some of nucleobases in water. Lhomme et al. showed the capacity of aryl-nucleobase conjugates to recognize certain nucleobases in water,[3] while Kimura et al. demonstrated that zinc(II) complexes of the macrocyclic tetraamine 1,4,7,10-tetraazacyclododecane (cyclen) have a unique propensity to bind with deprotonated imides like thymine and uracil, by forming non-covalent stable complexes in biologically relevant conditions.[4] Moreover, cyclens appended with aromatic rings such as acridine and ditopic receptors yielded binding constants for TMP and UMP up to K=10^7 M^{-1}.[5] Furthermore, some *cyclo*-bis-aromatic derivatives revealed selectivity toward certain nucleobases or basepairs due to the selective interactions of nucleobases with the linkers connecting aromatic subunits.[6] Previously prepared bis-phenanthridinium compounds have shown at the time the highest affinity toward nucleosides and nucleotides but not selectivity among studied nucleobases.[7,8] Intriguingly, comparison of the binding constants of monomer (order of magnitude Ks=10^2 M^{-1}) with calculated binding constants of bis-phenanthridinium analogs (order of magnitude Ks=10^6 M^{-1}) revealed that not only simultaneous involvement of two monomeric units in complex formation was present, which should give $Ks \approx 10^4$ M^{-1}, but also their cooperativity in binding. The difference between the expected $Ks \approx 10^4$ M^{-1} and the obtained $Ks \approx 10^6$ M^{-1} could be a consequence of hydrophobic effects (both, entropy- and enthalpy-driven),[9] pre-organisation of bis-phenanthridinium analogs suitable for nucleobase insertion (template effect),[10] as well as of the other interactions yielding significant template effect. Furthermore, previously reported phenanthridinium–nucleobase conjugates were not able to differentiate among selected nucleotides in aqueous medium, most likely due to the strong competition of bulk water with the expected hydrogen bonds between complementary nucleotide and nucleobase attached to the intercalator.[11–13] However, the same phenanthridinium–nucleobase conjugates interacted highly selectively with complementary polynucleotide sequences, most likely due to the polynucleotide hydrophobic environment, which allowed the formation of specific hydrogen bonds between nucleobase attached to intercalator and nucleobases of polynucleotide.[14,15]

The aforementioned results suggested that the nucleobase positioned within the hydrophobic cavity could recognize a complementary nucleotide by hydrogen bonding. To achieve both high

* Corresponding authors. Tel.: +385 1 45 71 210; fax: +385 1 46 80 195.
E-mail addresses: pianta@irb.hr, tomic@irb.hr (S. Tomić).

0040-4020/$ – see front matter © 2010 Elsevier Ltd. All rights reserved.
doi:10.1016/j.tet.2010.01.063

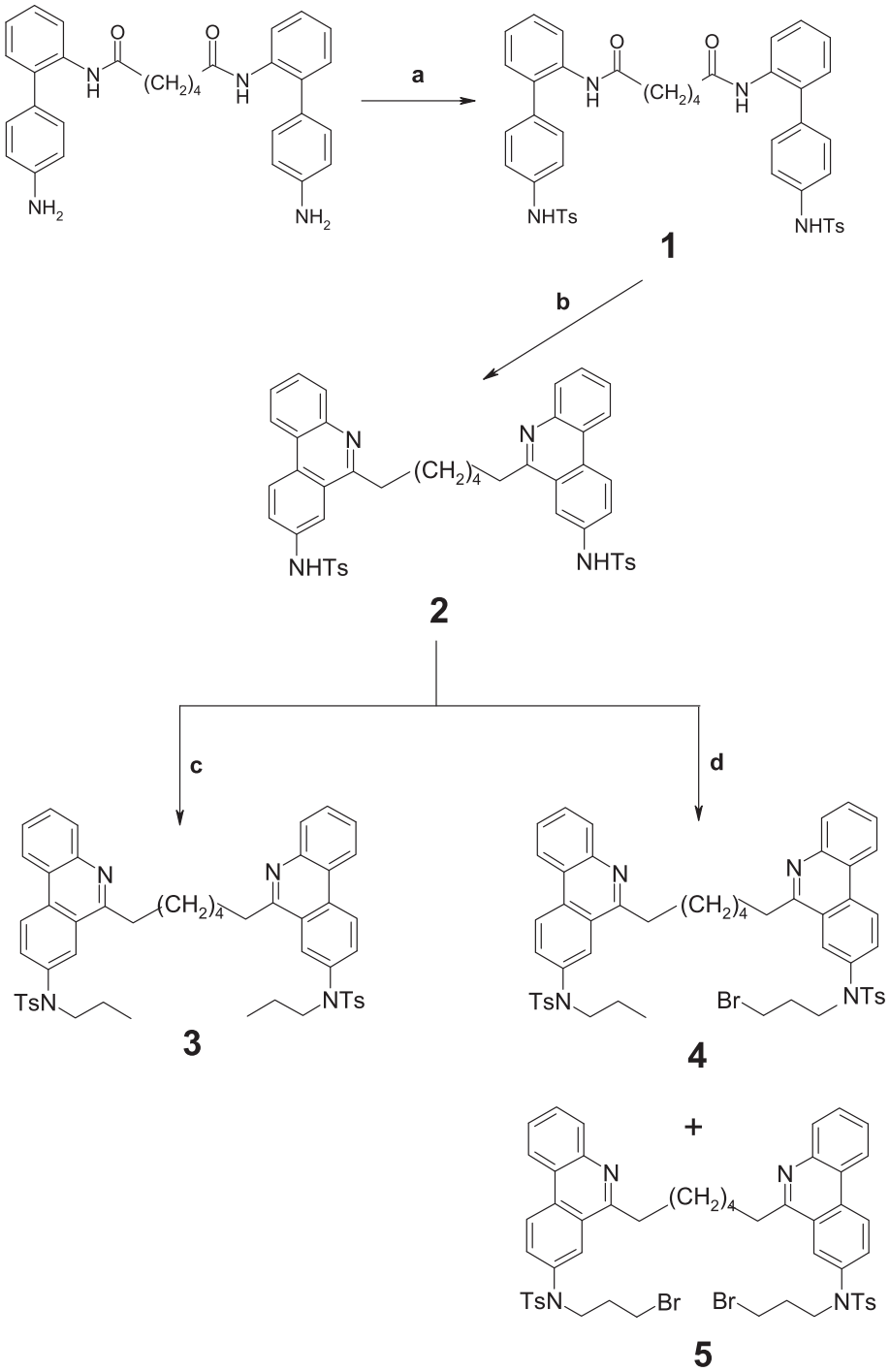

Scheme 1. The asymmetric (**4**) or symmetric (**3**, **5**) alkylation of tosylamino substituents of **2** by mono- and dibromopropane; (a) TsCl/pyridine/40–50 °C; (b1) $POCl_3$/120 °C (b2) NaOH/H_2O; (c) $Br(CH_2)_2CH_3$ (10 equiv)/K_2CO_3/DMF/Ar/rt (d1) $Br(CH_2)_2CH_3$ (1,5 equiv)/K_2CO_3/DMF/Ar/rt (d2) $Br(CH_2)_3Br$ (10 equiv)/K_2CO_3/DMF/Ar/rt.

stability and selectivity we used the bis-phenanthridinium skeleton, which, as previously reported,[8] forms highly stable complexes with nucleotides by aromatic stacking interactions, to which we covalently attached various nucleobases. Linkers between phenanthridinium units and between aromatic units were chosen to allow insertion of nucleobase between two phenanthridinium subunits, forming in this way a possible recognition site for complementary nucleotides within a hydrophobic cleft and additionally stabilising the targeted basepair by aromatic stacking interactions.

2. Results and discussion

2.1. Synthesis

Since it was not possible to covalently link nucleobases directly to the phenanthridine of previously studied bis-phenanthridinium derivatives,[7,16] novel synthetic strategy for building the bis-phenanthridinium skeleton had to be developed. The general strategy that was used for the synthesis of the novel bis-phenanthridinium-nucleobase conjugates **10**–**12** and reference

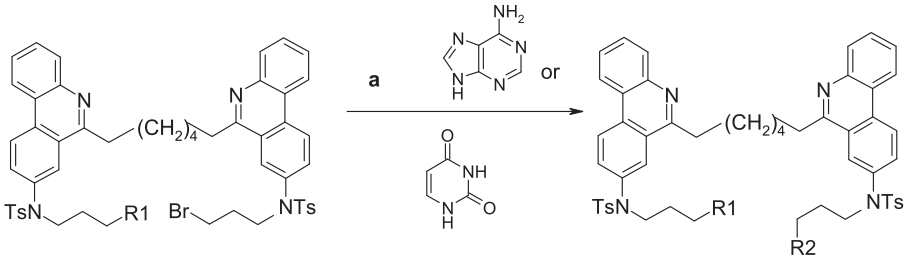

Scheme 2. Synthesis of conjugates **6**–**8**. (a) NaH/DMF/Ar/40–50 °C.

compound **9** comprised the asymmetric or symmetric alkylation of the amino substituents of bis-phenanthridine **2** by mono- and dibromopropane (Scheme 1), followed by the introduction of nucleobase at the other end of one or both alkyl linkers (Scheme 2), and subsequent deprotection of tosylated compounds (Scheme 3). Compound **1** was prepared starting from *N*,*N*′-bis-[(4′-amino)-2-biphenylyl]-octanediamide[16] that was tosylated in pyridine. The bis-phenanthridine **2** was obtained by the Morgan–Walls reaction[17] based on the central pyridine ring formation by intramolecular electrophilic cyclisation of the bis-biphenylyl **1** using $POCl_3$. Then, bis-phenanthridine **2** was alkylated with a large excess of mono-bromopropane to give symmetric alkylaminobis-phenanthridine **3**. To get the asymmetric product **4**, one of two tosylamino groups of **2** was alkylated in the first reaction step over 7 days in the dark and at room temperature, using a small excess (1.5 equiv) of 1-bromopropane. Subsequently, a large excess of potassium carbonate and 1,3-dibromopropane were added dropwise in situ, in order to obtain asymmetric compound **4**, while symmetric compound **5** was obtained as a side product after purification by TLC (Scheme 1).

The reaction of bromo-derivatives **4** and **5** with a large excess of uracil or adenine was performed under argon atmosphere at 40–50 °C in dry DMF in the presence of NaH, giving compounds **6**–**8**. Under these conditions the alkylation of uracil selectively occurred at the N1 position, while adenine was selectively alkylated at the N9 position (Scheme 2).

Tosyl-groups were removed by heating at 100 °C under acidic conditions, followed by neutralization using 5 M NaOH aqueous solution (Scheme 3). Compounds **9**–**12** were found to be sufficiently soluble in water under acidic conditions (pH 5).

2.2. Spectroscopy

The UV–vis spectra of compounds **9**–**12** are strongly pH dependent, exhibiting a one-step change at $pK_a \approx 6$, which was attributed to the protonation of the phenanthridine heterocyclic nitrogen.[11,18] Due to the poor solubility of examined compounds in neutral and basic conditions, all further measurements were performed at pH=5.0, with more than 90% of all compounds being in the protonated (phenanthridinium) form. The absorbance of compounds **9**–**12** was linearly dependent on the concentration within the $c=1\times10^{-6}$–4×10^{-5} mol dm^{-3} range (Table 1), while at higher concentrations aggregation of chromophores, as well as some precipitation occurred. The compounds **9**–**12** exhibited fluorescence emission (Table 1) proportional to the concentration of compound up to $c=5\times10^{-6}$ mol dm^{-3}. Excitation spectra monitored at emission maxima agree well with the corresponding UV–vis spectra.

A pronounced hypochromic effect of **9**–**12** absorption maxima in comparison to the monomer compound **Ph**–**C3** ([a]H, Table 1) is most likely the consequence of intramolecular aromatic stacking interactions. Furthermore, comparatively weak fluorescence of reference compound **9** is most likely caused by strong intramolecular aromatic stacking between phenanthridinium subunits (Table 1), while significantly stronger fluorescence of bis-phenanthridinium-nucleobase conjugates **10**–**12** (in comparison to **9**) could be the result of intramolecular un-stacking of phenanthridinium subunits caused by at least partial nucleobase insertion.

2.3. Interactions with nucleotides

Interactions of compounds **9**–**12** with nucleotides in aqueous medium were studied by UV–vis and fluorimetric titrations. Due to the low solubility of **9**–**12**, UV–vis titrations were performed using an immersion probe with 5 cm light path length, which allowed measurements at concentration range of 10^{-6} mol dm^{-3}, thus at experimental conditions comparable to fluorimetric titrations. It should be noted that UV–vis spectra were collected in the range λ=260–300 nm, at which both, **9**–**12** and also nucleotides absorb light, therefore for the processing of the titration-induced changes in complete spectral range multivariate analysis program was necessary (we applied Specfit).[19] It should be stressed that at λ>290 nm adenine and uracil (in contrast to guanine and cytosine) do not have an UV–vis spectra (for UV–vis spectra of nucleotides see Supplementary data) and therefore titration-induced changes in this part of **9**–**12** UV–vis spectra can be attributed only to the changes in the absorption properties of phenanthridinium chromophore. Titration with AMP and GMP yielded significantly stronger changes in the UV–vis spectrum (λ>290 nm) of the reference compound **9** in comparison to effects induced by UMP and CMP, most likely due to the larger aromatic surface of purine nucleobases in comparison to pyrimidines and consequently more efficient aromatic stacking interactions.

Intriguingly, titration with UMP induced a significantly stronger hypochromic effect in the UV–vis spectra (at λ>290 nm) of adenine conjugates **11** and **12**, if compared to reference compound **9** and uracil-conjugate **10** (Fig. 1). Even more interesting is the observation that titration with AMP induced a clear hyperchromic effect in the UV–vis spectra (at λ>290 nm) of adenine conjugates **11** and **12** (see, for example, Fig. 2), demonstrating that electronic absorption properties of phenanthridinium chromophores of **11** and **12** are significantly different upon complexation of UMP and AMP.

Changes in the UV–vis spectra at λ>290 nm of **9**–**12** upon titration with GMP and CMP were less informative due to the partial masking of changes by the intrinsic UV–vis spectra of nucleotides.

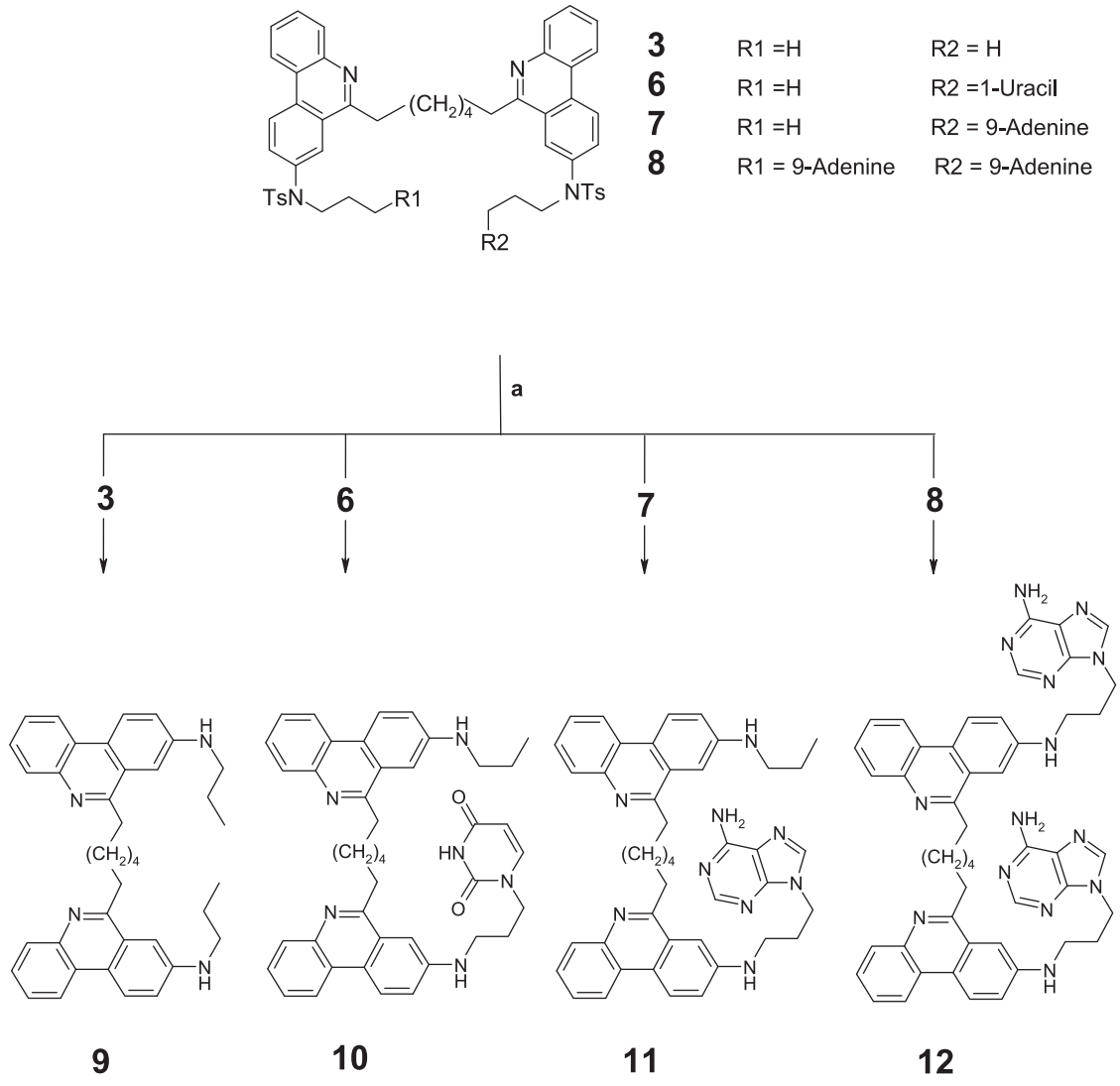

Scheme 3. Deprotection of compounds **3** and **6–8**. (a1) H_2SO_4/CH_3CO_2H/80–100 °C (a2) NaOH/H_2O.

Table 1
Molar extinction coefficients and absorption maxima of **9–12** and monomer compounds [c]**Ph–C3**, [c]**Ur–C3**, [c]**Ad–C3**, hypochromic effects (H)[a] of **9–12** in respect to monomer compounds. Fluorescence emission intensities at emission maxima of compounds **9–12**

	UV–vis			Fluorescence	
	λ_{max}/nm	ε ($mmol^{-1}\,cm^2$)	[a]H (%)	λ_{em}/nm	I_i[b]/I_2 (550 nm)
9	269	9269	85	552	1
10	275	25,497	62	565	19
11	270	16,436	75	560	14
12	273	30,526	55	558	31
[c]**Ph–C3**	277	29,282	—	547	[c,d]
[c]**Ur–C3**	268	9841	—	—	—
[c]**Ad–C3**	262	13,733	—	—	—

[a] (Na citrate/HCl buffer, pH=5.0, I=0.03 mol dm^{-3}), H (hypochromic effect)={[2×ε_{277nm} (**Ph–C3**)+n×ε_{277nm} (**Ur–C3** or **Ad–C3**)−ε_{277nm} (**9–12**)]/[2×ε_{277nm} (**Ph–C3**)+n×ε_{277nm} (**Ur–C3** or **Ad–C3**)]}×100; n=0 for compound **9**, n=1 for compounds **10**, **11**; n=2 for **12**.

[b] For all compounds c=2.2×10^{-6} mol dm^{-3}, λ_{exc}=270 nm; relative intensities calculated at λ=550 nm taking **9** as a reference.

[c] Published results.[11]

[d] Not possible to compare due to different experimental conditions.

However, fluorimetric titrations (Fig. 3) yielded more pronounced spectroscopic changes than UV–vis titrations and therefore binding constants (*Ks*) and stoichiometries of the complexes determined upon processing the titration data by Specfit[19] program are more accurate than those calculated from UV–vis titrations. Nevertheless, both methods yielded quite comparable *Ks* values and for all titrations the best fit was obtained for stoichiometry **9–12**/nucleotide=1:1 (Table 2).

The binding constants (Table 2) obtained for reference compound **9** and all studied nucleotides are comparable with those of previously studied phenanthridinium-based bis-intercalands and *cyclo*-bis-intercalands.[7] It should be stressed that monomer **Ph–C3** binds nucleotides predominantly by aromatic stacking interactions yielding log *Ks*≈2. Since compound **9** consists of two **Ph–C3** subunits linked by an inert aliphatic chain, if aromatic stacking interactions would be dominant in **9**/nucleotide complexes, the values of *Ks* (**9**/nucleotide)≈*Ks* (**Ph–C3**/nucleotide),[2] which are actually not the case (Table 2); the obtained values of *Ks* (**2**/nucleotide) are more than two orders of magnitude higher, suggesting the presence of a significant template effect.[7] The affinity of bis-

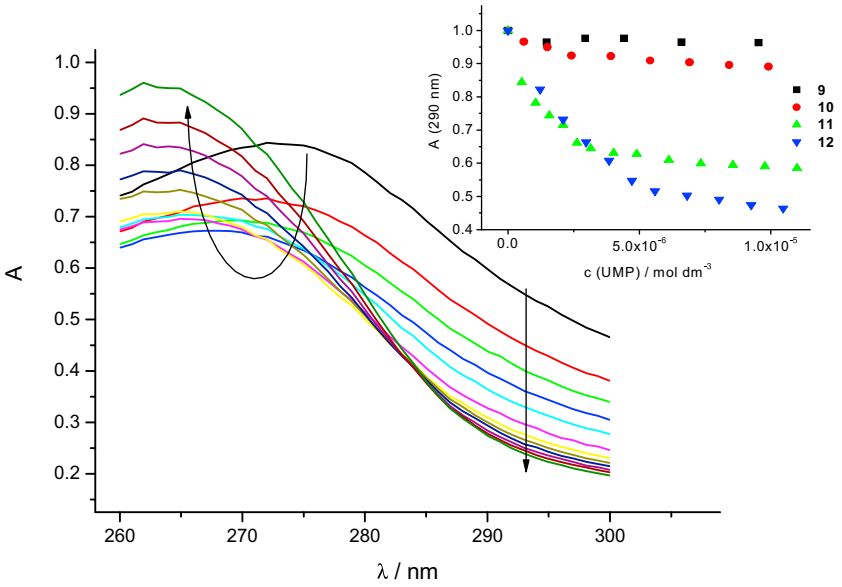

Figure 1. UV–vis titration of **12** with UMP (c(**12**)=2×10^{-6} mol dm^{-3}; c(UMP)=1.2×10^{-6}–12×10^{-6} mol dm^{-3}); Inset: changes in the UV–vis spectra (at λ=290 nm) of **9**–**12** (c=2×10^{-6} mol dm^{-3}) upon titration with UMP, done at pH=5.0 (Na cacodylate/HCl buffer, I=0.05 mol dm^{-3}).

phenanthridinium-nucleobase conjugates **10**–**12** toward most of the studied nucleotides is comparable to the reference compound **9** affinities. That is also pointing toward a significant template effect in respect to previously studied phenanthridinium-nucleobase conjugates,[11,12] as well as phenanthridinium-bis-nucleobase conjugates.[13]

Most intriguingly, the adenine-conjugate **11** binds complementary nucleotide UMP with the binding constant (*K*s **11**/UMP) an order of magnitude higher than any of the binding constants obtained for the reference compound **9** (*K*s **9**/nucleotide). Moreover, the affinity of **11** toward UMP is significantly higher than affinity of **11** toward other nucleotide mono-phosphates (AMP, GMP, CMP, Table 2, Fig. 3B). Such significantly stronger affinity points toward additional interactions between **11** and UMP (not present in the case of other nucleotide mono-phosphates).

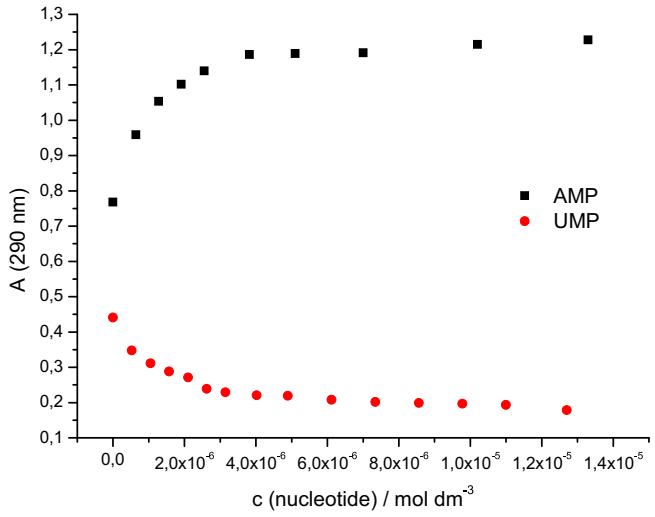

Figure 2. Changes in the UV–vis spectrum (at λ>290 nm) of **11** (c=2×10^{-6} mol dm^{-3}) upon titration with UMP (■) and AMP (●), done at pH=5.0 (Na cacodylate/HCl buffer, I=0.05 mol dm^{-3}).

2.4. Discussion of results of spectrophotometric titrations

The UV–vis spectrum of an aromatic moiety usually reveals a hypochromic effect upon stacking with another aromatic π–π system, although the intensity of hypochromic effect is not directly related to the binding constant. Therefore, the hypochromic effect of **9**–**12** compared to monomer **Ph**–**3** can be explained by intramolecular aromatic stacking of two phenanthridinium units, accompanied by additional stacking of covalently linked nucleobase (only for **10**–**12**). However, the fact that phenanthridinium chromophores of adenine conjugates **11** and **12** at λ>290 nm revealed a much stronger hypochromic effect upon UMP titration in comparison to reference **9** and uracil-conjugate **10** (Fig. 1) suggested more efficient overlapping of aromatic surfaces in the case of **11**/UMP and **12**/UMP complexes, whereby one of the possible explanations is formation of an adenine–UMP basepair within the lypophilic pocket between two phenanthridinium subunits. Moreover, such adenine–UMP basepair interactions within **11**/UMP and **12**/UMP complexes could be correlated to the observed opposite changes (hyperchromic effect) in the UV–vis spectra of adenine conjugates **11** and **12** at λ>290 nm upon titration with UMP and AMP (Fig. 2). Namely, the freedom of orientation of covalently bound adenine between two phenanthridinium subunits is very limited and basepair formation with AMP is hard to imagine. Moreover, the surface of such an adenine–adenine basepair would exceed the surface of phenanthridinium and therefore could not effectively yield better overlapping of aromatic surfaces in comparison to an uracil–adenine basepair. Therefore, it is most likely that AMP and covalently bound adenine compete for the binding sites within **11** and **12**, yielding as a final result a hyperchromic effect at λ>290 nm (UV–vis range of phenanthridinium chromophores).

An order of magnitude higher binding constant of **11**/UMP complex in comparison to any other **11**/nucleotide complex or **9**/nucleotide complex (Table 2) is also in line with the proposed adenine–UMP basepair formation. Assuming that hydrogen bonding is contributing to the selectivity of **11** toward UMP, the adenine of **11** should be positioned in a hydrophobic surrounding (e.g., between phenanthridinium subunits), within which water molecules are mostly excluded. Otherwise, competition of the extremely high

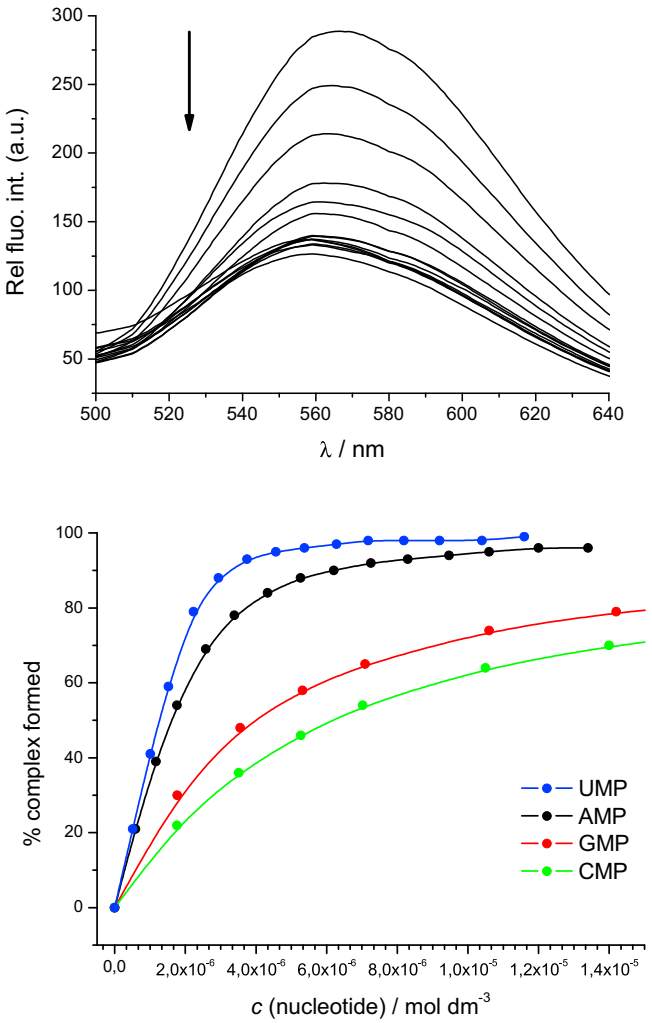

Figure 3. (A) Fluorimetric titration of **11** ($c=2\times10^{-6}$ mol dm^{-3}) with UMP; (B) percentage of formed **11**/nucleotide complex calculated by Specfit.[19]

excess of bulk water would not allow formation of hydrogen bonds between nucleobases, as previously noted for phenanthridinium–nucleobase conjugates.[11,12]

Since the aforementioned UV–vis and fluorimetric titrations cannot directly prove proposed adenine–UMP basepair formation, and low solubility of **9**–**12** hampered detailed studies by structurally more specific methods (NMR, crystallographic studies), we have investigated the possible conformations of such complexes by molecular modeling studies.

2.5. Molecular modeling

All studied molecules were prepared in both; extended and maximally folded shape with rings stacked conformations, solvated, energy optimised, and subjected to MD simulations (for details of MD simulations see section '4.3. Molecular modeling'). During the MD simulations the extended conformations folded and the stacked ones slightly unfolded. However the majority of molecules retained their folded (more or less stacking conformation), with no water molecules accommodated within the two phenanthridinium units (Fig. 4). Obtained structures are in accordance with the pronounced hypochromic effect of **9**–**12** absorption maxima (Table 1) in comparison to that of the reference compound **Ph–C3**, whereby the strongest hypochromic effect of **9** (if compared to nucleobase conjugates **10**–**12**) supports the insertion of a nucleobase between phenanthridinium subunits (as shown in Fig. 4). Apparently, the impact of multiple aromatic stacking interactions on the hypochromicity in the UV–vis spectrum is significant for the studied bis-phenanthridinium skeleton. The stacking interaction is the most efficient between two phenanthridinium subunits (**9**), insertion of another aromatic moiety decreases the stacking interaction intensity, whereby the effect of uracil, i.e., smaller aromatic moiety (**10**) insertion is in comparison with stacking of the adenine (**11**, **12**) being less favorable. Although the fluorescence of small molecules in water is a complex phenomenon and often cannot be directly correlated to structural properties, it is intriguing that the intensity of fluorescence emission of phenanthridinium units of all studied nucleobase conjugates is significantly stronger than that of compound **9** (Table 1), also supporting intramolecular interactions of nucleobases with fluorescence emitting chromophores.

Since the conformations presented in Figure 4 resemble to the molecular shape of a hydrophobic cavity in which there are no water molecules, we considered them to be excellent starting points for further modeling studies of the non-covalent complexes with nucleoside mono-phosphates AMP and UMP.

In the initial conformation of the **9**–AMP complex, used in MD simulations, adenine was inserted between two phenanthridinium units in a similar manner as obtained for covalently bound adenine-conjugate **11** during MD simulations (Fig. 4). Complexes **11**–UMP and **11**–AMP were built in a way to enable adenine from **11** and base from mono-phosphate to form hydrogen bonds (Figs. 6A and 7A).

The complexes were solvated in water and the systems were geometry optimised and subjected to molecular dynamics simulations for 8.5 ns. The initial orientations of the bis-

Table 2
Binding constants log *Ks* calculated from fluorimetric titrations and UV–vis titrations (in brackets) for **9**–**12**/nucleotide complexes[a,b]

[b]	**9**	**10**	**11**	**12**	**Ph–C3**
AMP	5–6[c] (5.60±0.11)	5.75±0.03 (≈5–6)[c]	6.34±0.06 (≈5–6)[c]	5.63±0.06 (≈5–6)[c]	1.73±0.02 (nd)
ADP	>6[c]	6.19±0.17	6.21±0.23	6.42±0.16	1.78±0.03
ATP	>6[c]	6.14±0.05	6.91±0.23	6.63±0.19	2.29±0.02
GMP	5–6[c] (5.73±0.15)	5.97±0.03 (≈5–6)[c]	5.45±0.04 [d]	5.55±0.08 [d]	1.72±0.09 (nd)
CMP	5–6[c] (5–6)[c]	5.69±0.04 [d]	5.24±0.04 [d]	5.48±0.07 (5–6)[c]	1.93±0.08 (nd)
UMP	5–6[c] (5–6)[c]	6.11±0.04 (5–6)[c]	6.89±0.11 (6.23±0.15)	5.86±0.09 (5–6)[c]	1.59±0.09 (nd)

[a] Titrations done at pH=5 (Na cacodylate/HCl buffer, I=0.05 mol dm^{-3}) and log *Ks* values are given for stoichiometry **9**–**12**/nucleotide=1:1.
[b] AMP^{2-}=adenosine mono-phosphate; GMP^{2-}=guanosine mono-phosphate; CMP^{2-}=cytidine mono-phosphate; UMP^{2-}=uridine mono-phosphate.
[c] Due to the small spectroscopic changes less than 10 data points were collected, allowing only estimation of binding constant.
[d] Small spectroscopic changes of complex compared to ligand and nucleotide resulted in linear change of absorbance, which hampered even estimation of the binding constant.

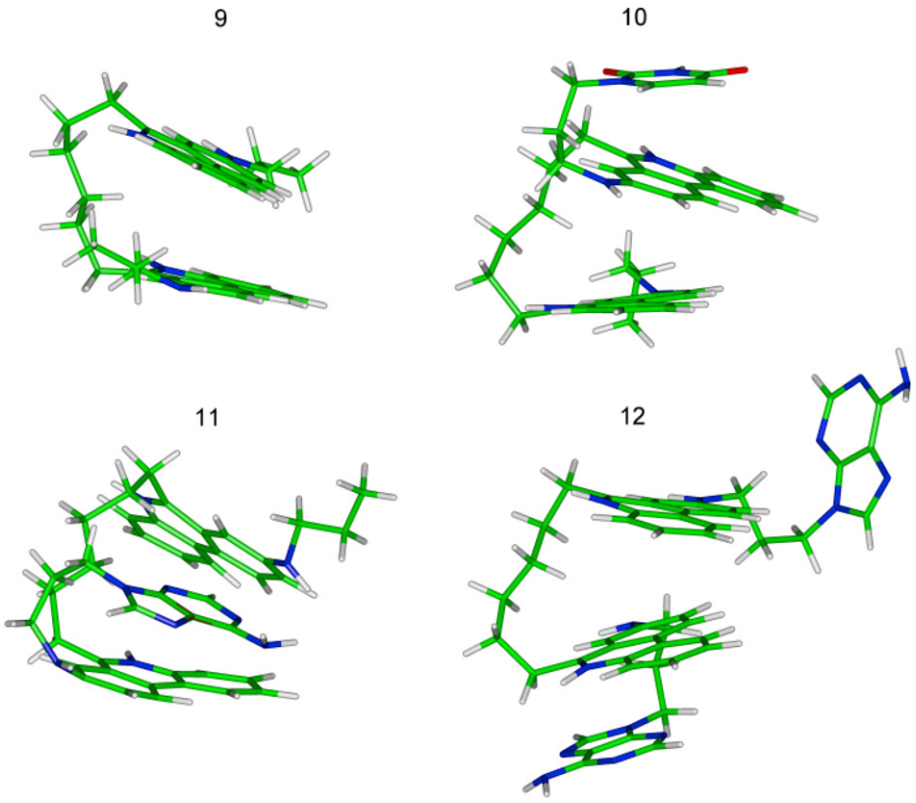

Figure 4. Conformations of studied compounds obtained by MD simulations.

phenanthridinium conjugates nucleobase and the nucleosides did not change significantly during the optimisation and the Watson–Crick (W–C) type of interaction was retained in **11**–UMP complex (Fig. 6A). However, during the MD simulation the conformations of the complexes changed (see, for example, Fig. 5). In comparison with the initial, optimized structures the simulation yielded less organized structure of **9**–UMP complex. The difference between the final structures of **9**–AMP and **9**–UMP complexes (Supplementary data) obtained upon MD simulation, clearly point out the importance of the size of aromatic part of nucleobase, whereby only larger purine nucleobase was able to form stable complex by insertion between the phenanthridinium subunits.

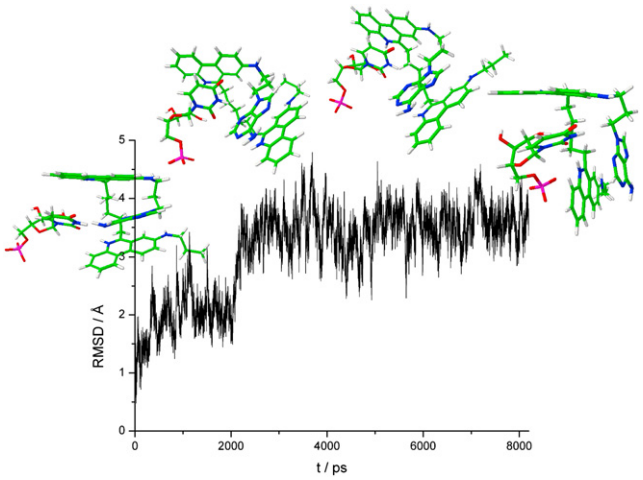

Figure 5. Conformation of the **11**–UMP complex significantly changed during MD simulation in water.

The **11**–UMP complex reorganized into the more compact form (Fig. 6B) stabilized by two intermolecular stacking interactions—face to face and face to edge between uracil and two Phen. Unit and one intramolecular stacking interaction (Phen. Unit—adenine). The hydrophobic pocket outlined by two perpendicularly oriented phenanthridinium units and the alkyl linker prevented water molecules to compete with uracil from UMP in forming two intermolecular hydrogen bonds: one with adenine and the other with phenanthridinium subunit. The potential energy of the final system is about 7% lower than that of the initial. Furthermore, stabilization due to solvation effects also increased during the MD simulation: the non-polar solvent-accessible surface area decreased for about 22% and the polar solvent-accessible surface area increased for about 6%.

The **11**–AMP complex (Fig. 7A) also reorganized into the more stable conformation during MD simulations (Fig. 7B). However the stabilisation due to the solvation effects is insignificant, i.e., the non-polar solvent-accessible surface area of the complex decreased by only about 8% and the polar solvent-accessible surface area decreased by about 4%.

The overall shape of the final **11**–AMP complex (Fig. 7B) is less compact (as can be seen from decrease of solvent-accessible surface area) and the overlapping of aromatic units is less pronounced in comparison to the **11**–UMP complex (Fig. 6B). The latter property could be correlated to the opposite changes in UV–vis titration experiments (Fig. 2); namely three aromatic stacking interactions between UMP and **11** could yield hypochromic effect with respect to free **11**, while less pronounced aromatic overlapping caused by addition of AMP to **11** could result in the hyperchromic effect.

3. Conclusions

The bis-phenanthridinium–adenine derivative **11** successfully combined the high affinity of previously known bis-intercalands[7]

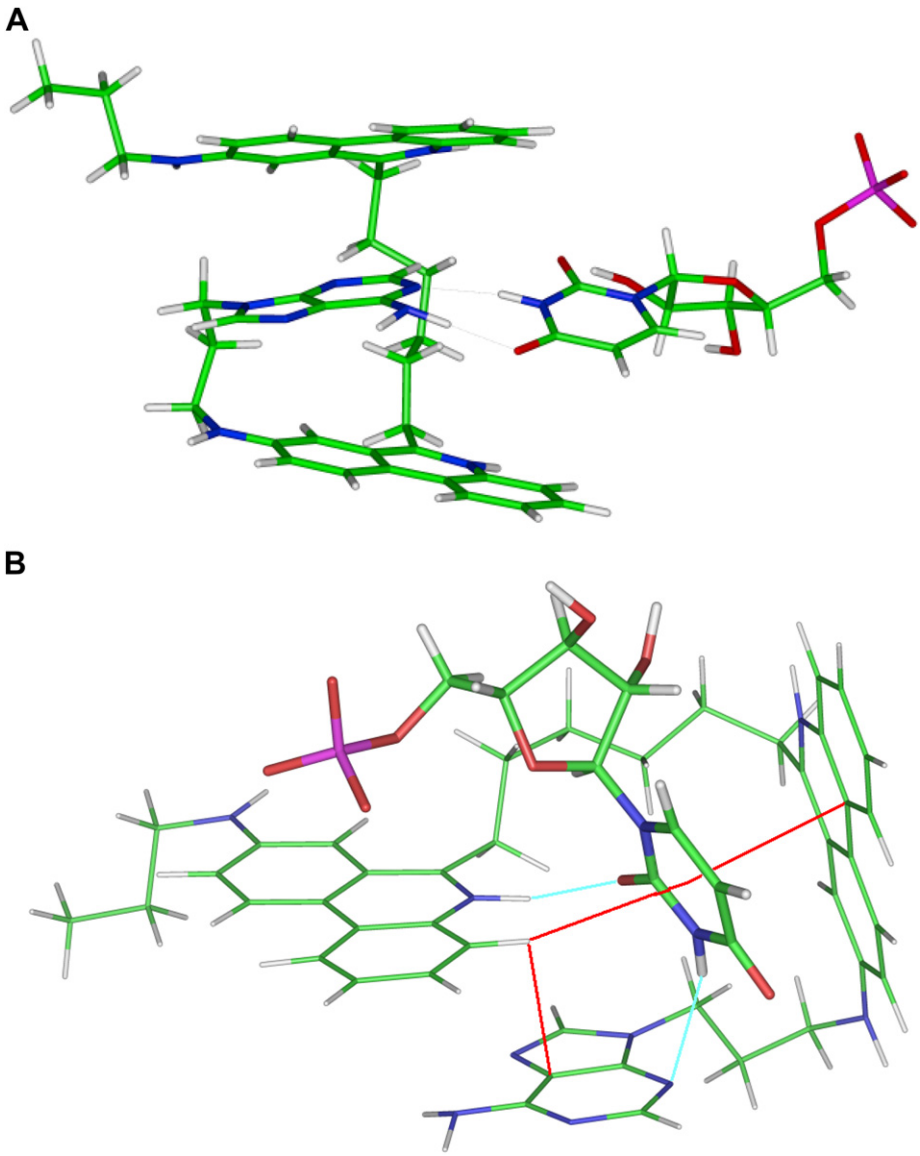

Figure 6. The starting conformation of **11**–UMP complex with the Watson–Crick type of H-bonds (A) changed to the conformation (B) in which the complex is stabilized by three intermolecular stacking interactions (—) and two intermolecular H-bonds (—).

toward nucleobases with selectivity toward complementary nucleotide (UMP). Molecular modeling studies suggest that selectivity of **11** toward UMP with respect to other nucleotides is most likely a consequence of organization of the **11**–UMP complex in the compact form stabilized by efficient intra- and intermolecular stacking interactions (as shown by hypochromic effect in UV–vis titration) as well as by intermolecular hydrogen bonds between uracil and **11**.

Other bis-phenanthridinium–nucleobase derivatives (**10** and **12**) were not able to distinguish between studied nucleotides significantly. The MD simulations of uracil-conjugate **10** as well as **9**–UMP complex suggest that uracil due to the small aromatic surface was not able to form a stable conformation in which it would simultaneously form stacking interactions with both phenanthridinium subunits and therefore failed to induce formation of the hydrophobic cavity necessary for hydrogen bonding recognition of nucleotides. On the other hand, two adenines attached to derivative **12** could compete with any nucleotide added, thus lowering the binding constant value.

Finally, the high affinity of novel compounds **9**–**12** toward nucleotides makes studies of their interactions with single stranded and double stranded DNA/RNA sequences highly promising, whereby selectivity of **11** toward UMP could be even more pronounced in a case of more hydrophobic poly U. In addition, other bis-phenanthridinium–nucleobase derivatives could also reveal selective affinity and/or spectroscopic sensing toward complementary DNA/RNA sequences. Furthermore, all studied compounds and especially derivative **9** are expected to show high affinity toward ds-DNA, and consequently pronounced biological activity, like many other bis-aromatic compounds.[20,21]

4. Experimental

4.1. General procedures

^{1}H and ^{13}C NMR spectra were recorded on Bruker Avance DRX 500 operating at 500 MHz. Chemical shifts (δ) are expressed in ppm, and J values in Hz. Signal multiplicities are denoted as s (singlet), d (doublet), t (triplet), ps. t. (pseudo triplet), q (quartet) and m (multiplet). The electronic absorption spectra of newly prepared compounds were measured on a Varian Cary 100 Bio spectrometer in quartz cuvettes (1 cm and

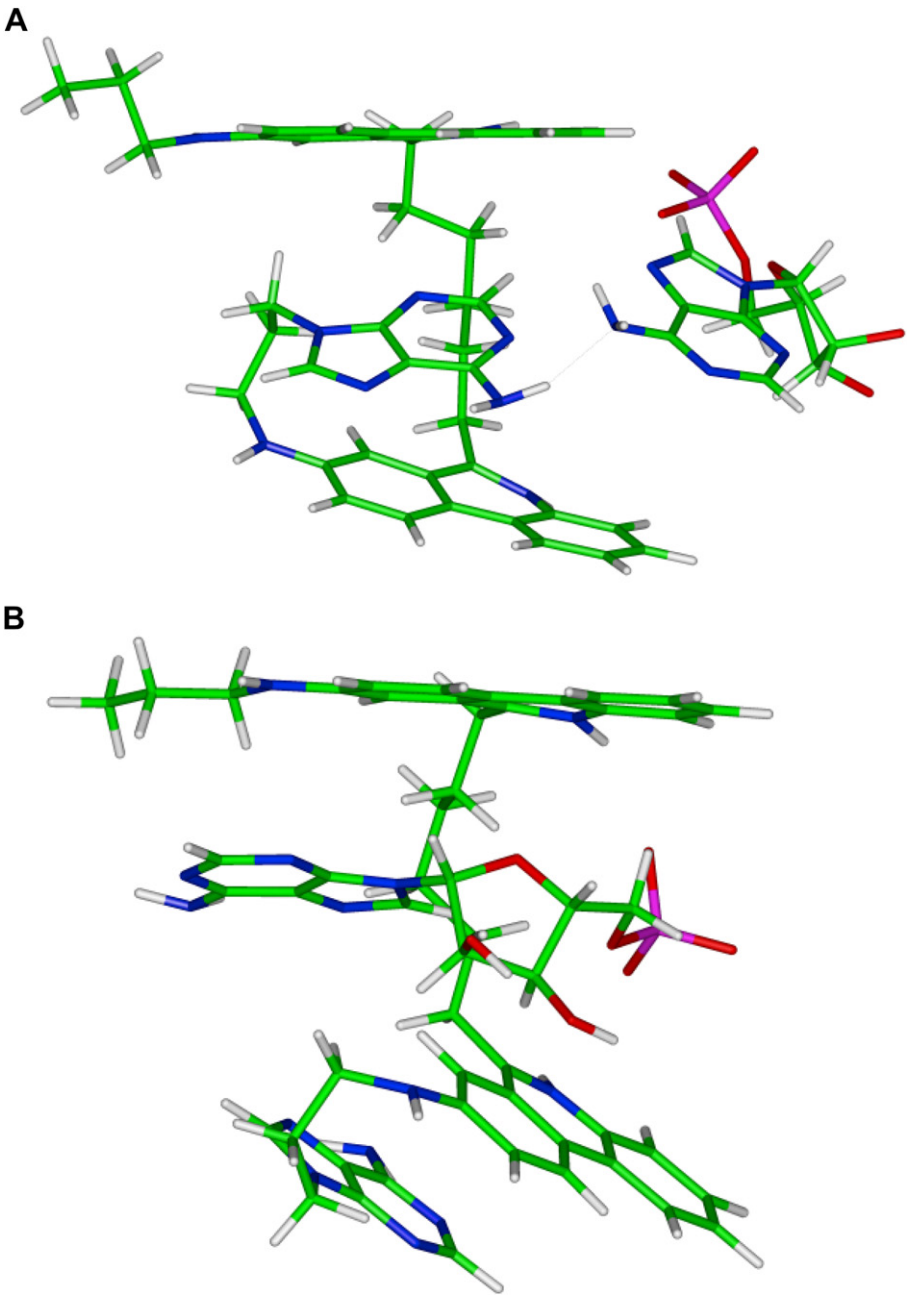

Figure 7. The starting conformation of **11**–AMP complex (A) changed to the conformation (B), in which covalently attached adenine was displaced by AMP from the cavity between two Phen. units.

10 cm). UV–vis titration were performed on a Varian Cary 100 Bio spectrometer and also on Varian Cary 50 using immersion probe with 5 cm light path length. IR spectra were recorded on a Perkin–Elmer 297 instrument using KBr pellets. Fluorescence spectra were recorded on Varian Cary Eclipse fluorimeter. Mass spectra were obtained using Applied Biosystems 4800 *Plus* MALDI TOF/TOF™ Analyzer. Preparative thin layer chromatography (TLC) was carried out using Kieselgel HF_{254} 'Merck'. Melting points were determined on Kofler apparatus and are uncorrected. All products were characterized by NMR, IR, ESI-MS or HRMS. Hygroscopic character of compounds yielded elemental analyses with non-stoichiometric amounts of water—however, since NMR spectra of final compounds were in accordance with other, previously prepared close analogs,[22] proposed structures are not questionable.

4.2. UV–vis and fluorescence measurements

Nucleotides were purchased from Sigma and Aldrich, and used without further purification. The measurements were performed in aqueous buffer solution (pH=5, I=0.05 mol dm^{-3}, sodium cacodylate/HCl buffer). Under the experimental conditions used (concentration of compounds **9**–**12**$\approx 10^{-6}$ mol dm^{-3}) the absorbance and fluorescence intensities of **9**–**12** were proportional to their concentrations. Spectroscopic titrations were performed at constant ionic strength (buffer, I=0.05 mol dm^{-3}) by adding portions of nucleotide solution into solution of the tested compound. Obtained data were corrected for dilution. UV–vis titrations were performed using immersion probe with 5 cm light path length, which allowed measurements at concentration range of 10^{-6} mol dm^{-3}, thus at experimental conditions comparable to fluorimetric titrations. It

should be noted that UV–vis spectra were collected in the range λ=260–300 nm, at which both, **9**–**12** and also nucleotides absorb light, therefore for the processing of the titration-induced changes in complete spectral range multivariate analysis program was necessary. In fluorimetric titrations, excitation wavelengths at λ_{max}=320 nm were used in order to avoid absorption of excitation light by added nucleotides and changes in emission at maxima were monitored. The binding constants and stoichiometries of complexes of **9**–**12** with nucleotides were calculated for the concentration range corresponding to ca. 20–80% complexation by non-linear least-square fitting program SPECFIT.[19]

4.3. Molecular modeling

Molecules were built using the module 'Builder' within the program InsightII,[23] and using the option 'Modify Torsion' the stacking conformation was prepared for each of the molecule. The crystal structure of AMP was separated from crystal structure of complex with PDB-id code 1Z6S. UMP was constructed using the crystal structure of AMP by replacing A with U. The replacement was done using the module 'Biopolymer' within the program InsightII. The AMBER ff03 force field of Duan et al.[24] and the general AMBER force field GAFF were used to obtain parameters for the bisphenanthridinium conjugates, nucleoside mono-phosphates, and water molecules. The tLeap module of AMBER 9 was used to obtain topology and coordinate files for molecules and complexes. Each molecule was placed in the center of an octahedron that was filled with TIP3P type water molecules; the water buffer of 8 Å was used. Besides water molecules, Cl− ions were added to neutralize the system when necessary Geometry optimization and molecular dynamics (MD) simulations were accomplished using the AMBER 9 program package.[25] The simulation was accomplished using Periodic Boundary Conditions (PBC). The Particle Mesh Ewald (PME) method was used for calculation of electrostatic interactions. In the direct space the pairwise interactions were calculated within the cutoff-distance of 11 Å. Before molecular dynamics (MD) simulations, the system was optimized using steepest descent and conjugate gradient methods, 1500 steps of each. After energy minimization, the system was equilibrated during 10 ps. During equilibration, the temperature was linearly increasing from 0 to 300 K and the volume was held constant. The equilibrated system was then subjected to at least 8.5 ns (UMP-**11** and AMP-**11**, 13.5 ns AMP-**9**) of productive unconstrained molecular dynamics simulation at constant temperature and volume (300 K). The time step during the simulation was 1 fs and temperature was held constant using Langevin dynamics with a collision frequency of 1 ps^{-1}.

The trajectories were visualized using the VMD 1.8.6 program. The RMSDs (root mean square deviations) between the initial conformation and those obtained during the MD simulation were calculated for each complex. The trajectories were divided into several stages (consisting of subsequent conformations with similar RMSD), and for each of this stage the average conformation was determined. The average conformations, as well as the final one, were energy minimized using the same procedure as for the initial one. The obtained conformations were visually compared using the InsightII software.

4.4. Synthesis of compounds

*4.4.1. N,N′-Bis-[(4′-tosylamino)-2-biphenylyl]-octanediamide (**1**).* A solution of tosyl-chloride (1.5 g, 6.71 mmol) in 15 ml of pyridine was added dropwise during 1 h to the ice-cold solution of *N,N′*-bis-[(4′-amino)-2-biphenylyl]-*octanediamide*[16] (690 mg, 1.3 mmol) in pyridine (15 ml). After addition was completed, the reaction mixture was heated at 50–60 °C during 4 h. Subsequently, the reaction mixture was allowed to cool and then poured into water. A light yellow solid precipitated. Recrystallization from methanol gave white solid **1** (780 mg, 70% yield). R_f (SiO_2, 5% MeOH in CH_2Cl_2)=0.31; mp 110–112 °C; ^{1}H NMR (DMSO-d_6) δ: 1.17 (br s, CH_2, 4H), 1.44 (br s, CH_2, 4H), 2.10 (t, CH_2, 4H, J=6.8 Hz), 2.32 (s, Ts–CH_3, 6H), 7.11 (d, Ts, 4H, J=8.6 Hz), 7.20–7.22 (m, Ar-H, 7H), 7.27–7.29 (m, Ar-H, 2H), 7.33–7.34 (m, Ar-H, 5H), 7.39–7.41 (m, Ar-H, 2H), 7.68–7.69 (m, Ar-H, 4H), 9.11 (s, NH–CO, 2H), 10.36 (s, NH–Ts, 2H); ^{13}C NMR (DMSO-d_6) δ: 21.09 (Ts–CH_3), 25.07, 28.57, 35.74, 119.42, 125.95, 126.85, 127.35, 127.63, 129.65, 129.84, 130.13, 134.49, 134.99, 136.15, 137.08, 137.16, 143.37, 171.61; IR (KBr) ν: 3464, 3246, 2924, 2853, 2366, 2345, 1647, 1524, 1508, 1458, 1445, 1385, 1339, 1325, 1227, 1157, 1092, 924, 841, 814, 764, 658, 573, 546 cm^{-1}. Anal. Calcd for $C_{46}H_{46}N_4O_6S_2$ (Mr 815.03 g mol^{-1}): C 67.72, H 5.96, N 6.87%. Found: C 67.36, H 5.48, N 6.70%.

*4.4.2. 1,6-Bis-(8-tosylaminophenanthridine-6-yl)-hexane (**2**).* Compound **2** was obtained by suspending *N,N′*-bis-[(4′-tosylamino)-2-biphenylyl]-suberamide **1** (2 g, 2.45 mmol) in 8 ml $POCl_3$ and heating the reaction mixture at 100–110 °C during 3 h. Mixture was allowed to cool and poured into ice, and afterward was made alkaline (pH=8–9) by addition of 3 M NaOH water solution. Yellow solid precipitated and was filtered and washed with water to give pale yellow powder (1.8 g, 94% yield); R_f (SiO_2, 10% MeOH in CH_2Cl_2)=0.52; mp 269–271 °C; ^{1}H NMR (DMSO-d_6) δ: 1.52 (br s, CH_2, 4H), 1.78 (br s, CH_2, 4H), 2.17 (s, Ts–CH_3, 6H), 3.18 (t, CH_2, 4H, J=7.7 Hz), 7.22 (d, Ts, 4H, J=8.2 Hz), 7.59–7.66 (m, Phen-2, Phen-3, Phen-4, 6H), 7.68 (d, Ts, 4H), 7.93–7.95 (m, Phen-7, Phen-9, 4H), 8.58 (dd, Phen-1, 2H, J_{1-3}=0.9 Hz, J_{1-2}=8.2 Hz), 8.70 (d, Phen-10, 2H, J_{9-10}=9.0 Hz), 10.68 (s, NH–Ts, 2H) ppm; ^{13}C NMR (DMSO-d_6) δ: 20.80 (Ts–CH_3), 28.46, 29.16, 35.48, 114.67, 122.15, 122.90, 123.68, 124.34, 125.09, 126.63, 126.71, 128.21, 129.08, 129.65, 129.97, 136.63, 142.58, 143.29, 160.85, 174.64 ppm; IR (KBr) ν: 3275, 3067, 2934, 2858, 2363, 2345, 1618, 1576, 1535, 1491, 1448, 1389, 1348, 1242, 1161, 1092, 953, 895, 814, 762, 669, 575, 544, 473, 459 cm^{-1}; (MALDI/TOF-HRMS) m/z: 779.2695 (calcd for $C_{46}H_{42}N_4O_4S_2$: 779.2720).

*4.4.3. 1,6-Bis-[8-(propyltosylamino)phenanthridine-6-yl]-hexane (**3**).* 1-Bromopropane (234 μl; 257 mmol; 20 equiv) and K_2CO_3 (266 mg; 1.93 mmol, 20 equiv) were suspended in dry DMF (10 ml). To this suspension, a solution of 1,6-bis-(8-tosylaminophenanthridine-6-yl)-hexane (**2**) (100 mg; 0.128 mmol) in dry DMF (5 ml) was added dropwise during 10 min and the reaction mixture was stirred for 4 days under argon atmosphere at room temperature. Water (70 ml) and CH_2Cl_2 (70 ml) were added to this suspension, the water layer was washed twice with CH_2Cl_2, organic extracts were dried over Na_2SO_4, and evaporated, yielding a brown oil. The oily residue was triturated with water to give a light brown precipitate that was filtered (71 mg, 64%), washed with water and dried, and used without further purification. Pure compound **2** was obtained by TLC (SiO_2, 2% MeOH in CH_2Cl_2, R_f=0.54) as a white solid, additionally recrystallized from MeOH; mp 187–189 °C; ^{1}H NMR ($CDCl_3$) δ: 0.93 (t, CH_3, 6H, J=7.3 Hz), 1.46–1.53 (m, CH_2–hexylene chain, CH_2–propyl chain, 8H), 1.85 (br s, CH_2–hexylene chain, 4H), 2.41 (s, Ts–CH_3, 6H); 3.21 (t, CH_2–hexylene chain, 4H, J=7.6 Hz), 3.65 (t, NCH_2, 4H, J=7.0 Hz), 7.23 (d, Ts, 4H, J=8.1 Hz), 7.45 (d, Ts, 4H), 7.54 (dd, Phen-9, 2H, J_{7-9}=1.9 Hz, J_{9-10}=8.7 Hz), 7.64 (t, Phen-2, 2H), 7.73 (t, Phen-3, 2H), 7.87 (d, Phen-7, 2H), 8.12 (d, Phen-4, 2H, J_{3-4}=8.0 Hz), 8.50 (d, Phen-1, 2H, J_{1-2}=8.0 Hz), 8.59 (d, Phen-10, 2H) ppm; ^{13}C NMR ($CDCl_3$) δ: 9.93 (CH_3), 20.47 (Ts–CH_3), 20.53 (CH_2–propyl chain), 28.06 (CH_2–hexylene chain), 28.58 (CH_2–hexylene chain), 34.50 (CH_2–hexylene chain), 51.18 (NCH_2), 120.90 (Phen-10), 121.99, 123.39 (Phen-1), 125.05 (Phen-7), 125.50, 126.59 (Ts), 127.05, 127.87 (Phen-3), 128.28, 128.40 (Ts), 128.63 (Phen-4), 129.81, 134.01, 142.46 ppm; IR (KBr) ν: 3425, 3065, 2961, 2932, 2874, 2858, 2363, 2345, 1599, 1572, 1528, 1479, 1458, 1344, 1238,

1213, 1167, 1090, 1074, 1020, 964, 872, 812, 766, 725, 708, 667, 642, 582, 550 cm^{-1}. Anal. Calcd for $C_{52}H_{54}N_4O_4S_2$ (Mr=863.16): C 72.36, H 6.31, N 6.49%. Found: C 72.05, H 6.22, N 6.54%; (MALDI/TOF-HRMS) *m/z*: 863.3644 (calcd for $C_{52}H_{54}N_4O_4S_2$: 836.3659).

*4.4.4. 1-[8-(3-Bromopropyltosyl)aminophenanthridine-6-yl]-6-[8-(propyltosyl)aminophenanthridine-6-yl]-hexane (**4**).* 1-Bromopropane (56 μl; 0.617 mmol; 1.6 equiv) and K_2CO_3 (133 mg; 0.964 mmol, 2.5 equiv) were suspended in dry DMF (10 ml). To this suspension, a solution of 1,6-bis-(8-tosylaminophenantridine-6-yl)-hexane (**2**) (300 mg; 0.386 mmol) in dry DMF (5 ml) was added dropwise over 10 min and the reaction mixture was stirred for 7 days under argon atmosphere at room temperature. Then, 1,3-dibromopropane (525 μl, 5.14 mmol, 13 equiv) and K_2CO_3 (533 mg; 3.86 mmol, 10 equiv) were added to the reaction mixture, and stirred for 2 days under argon atmosphere at room temperature. Water (70 ml) and CH_2Cl_2 (70 ml) were added to this suspension, the water layer was washed twice with CH_2Cl_2, organic extracts were dried over Na_2SO_4, and evaporated, yielding brown oil. The oily residue was triturated with water to give 826 mg of light brown precipitate that was filtered (160 mg, 44%), washed with water and dried. Pure compound **4** was obtained by TLC (SiO_2, 2% MeOH in CH_2Cl_2, R_f=0.54) as white solid (160 mg, 44%); mp 198–200 °C; ^{1}H NMR ($CDCl_3$) δ: 0.92 (t, CH_3, 3H, J=7.4 Hz) 1.44–1.53 (m, CH_2–hexylene chain, CH_2–propyl chain, 6H), 1.84 (br s, CH_2–hexylene chain, 4H), 2.08 (m, CH_2–propylene chain, 2H), 2.40 (s, Ts–CH_3, 6H), 3.22 (t, CH_2–hexylene chain, 4H, J=6.2 Hz), 3.45 (t, CH_2Br, 2H, J=6.4 Hz), 3.64 (t, NCH_2–propyl chain, 2H, J=7.0 Hz), 3.83 (t, NCH_2–propylene chain, 2H, J=6.6 Hz), 7.22 (d, Ts, 4H, J=8.0 Hz), 7.43 (m, Ts, 4H), 7.51–7.54 (m, Phen-9, 2H), 7.63 (m, Phen-2, 2H), 7.73 (t, Phen-3, 2H), 7.85–7.89 (m, Phen-7, 2H), 8.12 (d, Phen-4, 2H, J_{3-4}=7.8 Hz), 8.49 (d, Phen-1, 2H, J_{1-2}=7.6 Hz), 8.56–8.60 (m, Phen-10, 2H) ppm; ^{13}C NMR ($CDCl_3$) δ: 11.03 (CH_3), 21.52 (Ts–CH_3), 21.62, 29.19, 29.25, 29.57, 29.85, 31.71, 49.26, 52.24, 76.79, 77.00, 77.21, 122.03, 123.02, 123.12, 123.54, 123.77, 125.30, 125.36, 125.96, 126.06, 126.25, 126.36, 126.90, 127.65, 127.72, 129.25, 129.51, 129.61, 132.23, 132.37, 134.53, 135.06, 138.17, 143.60, 143.92, 161.72, 161.82 ppm; IR (KBr) ν: 3452, 2926, 2854, 2363, 2345, 1684, 1647, 1541, 1508, 1340, 1163, 1090, 964, 812, 766, 669, 582, 548, 473 cm^{-1}; (MALDI/TOF-HRMS) *m/z*: 941.2756 (calcd for $C_{52}H_{53}BrN_4O_4S_2$: 941.2764).

*4.4.5. 1,6-Bis-[8-(3-bromopropyltosylamino)phenanthridine-6-yl]-hexane (**5**).* Compound (**5**) was obtained as a side product during preparation of **4** as a white powder (30 mg, 8% yield), R_f (SiO_2, 2% MeOH in CH_2Cl_2)=0.25; mp 205–209 °C; ^{1}H NMR ($CDCl_3$) δ: 1.54 (br s, Phen-CH_2, 4H), 1.85 (br s, CH_2–hexylene chain, 4H), 2.07 (t, CH_2, 2H, J=6.4 Hz), 2.41 (s, Ts–CH_3, 6H), 3.24 (br s, CH_2–hexylene chain, 4H), 3.45 (t, Br–CH_2, 4H, J=6.9 Hz) 3.84 (t, NCH_2, 4H, J=6.9 Hz), 7.22 (d, Ts, 4H, J=8.0 Hz), 7.42 (d, Ts, 4H), 7.53 (d, Phen-9, 2H, J_{9-10}=8.8 Hz), 7.64 (m, Phen-2, 2H), 7.73 (m, Phen-3, 2H), 7.88 (s, Phen-7, 2H), 8.15 (br s, Phen-4, 2H), 8.49 (d, Phen-1, 2H, J_{1-2}=8.2 Hz), 8.58 (d, Phen-10, 2H) ppm; ^{13}C NMR ($CDCl_3$) δ: 21.53, 29.12, 29.59, 29.83, 31.76, 48.21, 49.29, 122.03, 123.01, 123.74, 125.45, 126.00, 126.77, 126.80, 127.74, 129.16, 129.60, 130.47, 132.33, 134.67, 138.15, 143.89, 161.65 ppm; IR (KBr) ν: 3447, 3065, 3032, 2926, 2854, 2365, 2345, 1717, 1653, 1541, 1458, 1346, 1242, 1163, 1092, 949, 812, 764, 725, 708, 667, 582, 548, 419, 397 cm^{-1}; (MALDI/TOF-HRMS) *m/z*: 1019.1891 (calcd for $C_{52}H_{52}Br_2N_4O_4S_2$: 1019.1869).

*4.4.6. 1-[8-(3-(Urac-1-il)propyltosyl)aminophenanthridine-6-yl]-6-[8-(propyltosyl)aminophenanthridine-6-yl]hexane (**6**).* Uracil (107 mg; 0.955 mmol, 10 equiv) that was previously dried, and NaH (38 mg, 60% w/w, 0.955 mmol, 10 equiv) were suspended in dry DMF (5 ml) and stirred during 1 h in argon atmosphere at room temperature. To this suspension, a solution of 1-[8-(3-bromopropyltosyl)aminophenanthridine-6-yl]-6-[8-(propyltosyl)aminophenanthridine-6-yl]-hexane **4** (90 mg; 0.095 mmol) in dry DMF (10 ml) was added dropwise and the reaction mixture was stirred during 48 h under argon atmosphere at 50 °C. Then, water (70 ml) and CH_2Cl_2 (70 ml) were carefully added to this suspension. The water layer was washed twice with CH_2Cl_2, organic extracts were dried over Na_2SO_4 and evaporated, yielding oily residue that was triturated with water to give 95 mg of white precipitate. The precipitate was filtered, washed with water and dried; and then purified by TLC (SiO_2, 10% MeOH in CH_2Cl_2, R_f=0.55). Compound **6** was obtained as white solid (35 mg, 37% yield); mp 200–203 °C; ^{1}H NMR ($CDCl_3$) δ: 0.90 (t, CH_3, 3H, J=7.8 Hz), 1.52 (m, CH_2–hexylene chain, CH_2–propyl chain, 6H), 1.84 (m, CH_2–hexylene chain, CH_2–propylene chain, 6H), 2.39 (s, Ts–CH_3, 6H), 3.19–3.24 (m, CH_2–hexylene chain, 4H) 3.62 (t, $NTsCH_2$–propyl chain, 2H, J=6.7 Hz), 3,72 (t, $NTsCH_2$–propylene chain, 2H, J=6.3 Hz), 3.85 (t, uracil-NCH_2–propylene chain, 2H, J=6.70 Hz), 5.66 (d, uracil-5, 1H, J_{5-6}=7.8 Hz), 7.21 (d, Ts, 4H, J=8.1 Hz), 7.31 (d, uracil-6, 1H), 7.36–7.46 (m, Ts, Phen-9, 5H), 7.51 (dd, Phen-containing-base-9, 1H, J_{7-9}=1.9 Hz, J_{9-10}=8.8 Hz), 7.59–7.74 (m, Phen-2, Phen-3, 4H), 7.83 (d, Phen-containing-base-7, 1H), 7.94 (d, Phen-7, 1H), 8.10 (d, Phen-4, 2H, J_{3-4}=7.3 Hz), 8,47 (d, Phen-1, 2H, J_{1-2}=8.1 Hz), 8.54 (d, Phen-10, 1H, J_{9-10}=8.9 Hz), 8.58 (d, Phen-containing-base-10, 1H), 8.78 (s, U-NH, 1H) ppm; ^{13}C NMR ($CDCl_3$) δ: 11.23 (CH_3), 21.73 (Ts–CH_3), 21.75 (Ts–CH_3), 21.81 (CH_2–propyl chain), 27.41 (CH_2–propylene chain), 29.21 (CH_2–hexylene chain), 29.76 (CH_2–hexylene chain), 36.05 (CH_2–hexylene chain), 46.51 (uracil–NCH_2–propylene chain), 47.69 ($NTsCH_2$–propylene chain), 52.35 ($NTsCH_2$–propyl chain), 102.27 (uracil-5), 114.76, 121.30, 122.22 (Phen-1), 122.23 (Phen-1), 123.1, 123.29, 123.7 (Phen-10), 124.1 (Phen-10), 125.69, 126.11, 126.85, 126.99, 127.84, 127.95, 129.44, 129.72, 129.87, 132.35, 132.70, 134.27, 135.27, 137.45, 143.8, 144.35, 145.24 (uracil-6), 150.74, 161.75, 163.51 ppm; IR (KBr) ν:3462, 2928, 2853, 2361, 2343, 1686, 1647, 1541, 1508, 1458, 1385, 1340, 1159, 1092, 812, 766, 723, 669, 584, 546 cm^{-1}; (MALDI/TOF-HRMS) *m/z*: 973.3742 (calcd for $C_{56}H_{56}N_6O_6S_2$: 973.3776).

*4.4.7. 1-[8-(9-(Aden-1-yl)propyltosyl)aminophenanthridine-6-yl]-6-[8-(propyltosyl)aminophenanthridine-6-il]hexane (**7**).* Compound **7** was obtained as described for **6**; 1-[8-(3-bromopropyltosyl)aminophenanthridine-6-yl]-6-[8-(propyltosyl)aminophenanthridine-6-yl]-hexane **4** (130 mg; 0.138 mmol), adenine (187 mg; 1.38 mmol, 10 equiv), and NaH (55 mg, 60% w/w, 1.38 mmol, 10 equiv) in dry DMF (10+10 ml) gave white powder **7** (50 mg, 36% yield), R_f (SiO_2, 10% MeOH in CH_2Cl_2)=0.48; mp 184–186 °C; ^{1}H NMR ($CDCl_3$) δ: 0.88 (t, CH_3, 3H, J=7.3 Hz), 1.45 (ps q CH_2–propyl chain, 2H), 1.51 (br s, CH_2–hexylene chain, 4H), 1.83 (br s, CH_2–hexylene chain, 4H), 2.05 (br s, CH_2–propylene chain, 2H), 2.36 (s, Ts–CH_3, 3H), 2.37 (s, Ts–CH_3, 3H), 3.19 (m, CH_2–hexylene chain, 4H), 3.61 (t, $NTsCH_2$–propyl chain, 2H, J=7.0 Hz), 3.68 (t, $NTsCH_2$–propylene chain, 2H, J=5.9 Hz), 4.30 (t, adenine–NCH_2–propylene chain, 2H, J=6.3 Hz), 5.80 (br s, adenine–NH_2, 2H), 7.16–7.19 (m, Ts, 4H), 7.34 (d, Ts, 2H, J=7.9 Hz), 7.42 (d, Ts-Phen-containing-base-, 2H, J=8.0 Hz), 7.45 (d, Phen-containing-base-9, 1H, J_{9-10}=8.6 Hz), 7.48 (d, Phen-9, 1H, J_{9-10}=8.7 Hz), 7.57 (ps. t., Phen-containing-base 2, 1H), 7.60 (ps. t., Phen-2, 1H), 7.65 (ps. t., Phen-containing-base-3, 1H), 7.70 (ps. t., Phen-3, 1H), 7.82 (s, Phen-containing-base-7, 1H), 7.86 (s, adenine-8, 1H), 7.89 (s, Phen-7, 1H), 8.06 (d, Phen-containing-base-4, 1H, J_{3-4}=8.0 Hz), 8.08 (d, Phen-4, 1H, J_{3-4}=8.0 Hz), 8.21 (s, adenine-2, 1H), 8.42 (d, Phen-containing-base-1, 1H, J_{1-2}=8.0 Hz), 8.46 (d, Phen-1, 1H, J_{1-2}=8.1 Hz), 8.50 (d, Phen-containing-base-10, 1H), 8.55 (d, Phen-10, 1H) ppm; ^{13}C NMR ($CDCl_3$) δ: 11.25 (CH_3), 21.72 (Ts–CH_3), 21.89 (CH_2–propyl chain), 28.57 (CH_2–propylene chain), 29.17 (CH_2–hexylene chain), 29.25 (CH_2–hexylene chain), 29.80 (CH_2–hexylene chain), 29.85 (CH_2–hexylene chain), 36.16 (CH_2–hexylene chain), 36.23 (CH_2–hexylene chain), 41.20 (adenine–NCH_2–propylene chain), 47.94 ($NTsCH_2$–propylene chain), 52.52 ($NTsCH_2$–

propyl chain), 122.20 (Phen-containing-base-1), 122.25 (Phen-1), 123.15, 123.28, 123.67 (Phen-containing-base-10), 124.04 (Phen-10), 125.75, 125.80, 126.16 (Phen-containing-base-7), 126.61 (Phen-7), 126.81 (Phen-containing-base-2), 126.92 (Phen-2), 127.93 (Ts), 127.99 (Ts), 129.16 (Phen-containing-base-3), 129.36 (Phen-3), 129.71 (Ts), 129.80 (adenine-8), 129.84 (Ts), 129.91 (Phen-containing-base-4), 130.04 (Phen-4), 130.47 (Phen-containing-base-9), 130.54 (Phen-9), 132.31, 132.65, 134.62, 135.50, 137.74, 138.28, 143.76, 144.16, 144.24, 144.29, 152.98 (adenine-2), 155.64, 161.69, 161.88 ppm; IR (KBr) ν: 3448, 2959, 2932, 2856, 2361, 2343, 1653, 1541, 1508, 1458, 1340, 1157, 1090, 1072, 951, 812, 762, 723, 706, 665, 582, 548 cm^{-1}; (MALDI/TOF-HRMS) m/z: 996.4083 (calcd for $C_{57}H_{57}N_9O_4S_2$: 996.4047).

*4.4.8. 1,6-Bis-[8-(3-(aden-9-yl)propyltosylamino)phenanthridine-6-yl]-hexane (**8**).* Compound (**8**) was obtained as described for **6**; 1,6-bis-[8-(3-bromopropyltosylamino)phenanthridine-6-yl]-hexane **5** (25 mg; 0.024 mmol), adenine (40 mg; 0.29 mmol, 10 equiv) and NaH (12 mg, 60% w.w., 0.29 mmol, 10 equiv) in dry DMF (5+5 ml) gave white powder **8** (20 mg, 70% yield), R_f (SiO_2, 10% MeOH in CH_2Cl_2)=0.28; mp 151–155 °C; ^{1}H NMR ($CDCl_3$) δ: 1.53 (br s, CH_2–hexylene chain, 4H), 1.84 (br s, CH_2–hexylene chain, 4H), 2.06 (t, CH_2–propylene chain, 4H, J=6.2 Hz), 2.38 (s, Ts–CH_3, 6H), 3.22 (t, Phen-CH_2–hexylene chain, 4H, J=7.7), 3.63 (t, NTsCH_2–propylene chain, 4H, J=6.0 Hz), 4,33 (t, adenine–NCH_2–propylene chain, 4H, J=6.3 Hz), 6.41 (br s, adenine–NH_2, 4H), 7.19 (d, Ts, 4H, J=8.1 Hz), 7.36 (d, Ts, 2H, J=8.2 Hz), 7.43 (dd, Phen-9, 2H, J_{7-9}=2.0 Hz, J_{9-10}=8.8 Hz), 7.61 (t, Phen-2, 2H), 7.70 (t, Phen-3, 2H), 7.89 (s, Phen-7, adenine-8, 4H), 8.09 (dd, Phen-4, 2H, J_{2-4}=1.0 Hz, J_{3-4}=8.1 Hz), 8.18 (s, adenine-2, 2H), 8.45 (d, Phen-1, 2H, J_{1-2}=7.5 Hz), 8.54 (d, Phen-10, 2H) ppm; ^{13}C NMR ($CDCl_3$) δ: 21.58 (Ts–CH_3), 28.14, 29.03, 29.52, 29.70, 35.93. 41.04, 47.46, 122.04, 122.87, 123.85, 125.51, 126.34, 126.76, 127.72, 129.21, 129.66. 129.80, 132.38, 134.09, 137.29, 143.90, 144.12, 152.44, 155.51, 161.62 ppm; IR (KBr) ν: 3421, 2922, 2851, 2363, 2345, 1647, 1597, 1574, 1475, 1420, 1385, 1340, 1304, 1244, 1159, 1109, 1088, 991, 935, 872, 814, 764, 725, 698, 667, 582, 544 cm^{-1}; (MALDI/TOF-HRMS) m/z: 1129.4405 (calcd for $C_{62}H_{60}N_{14}O_4S_2$: 1129.4435).

*4.4.9. 1,6-Bis-[8-(propylamino)phenanthridine-6-yl]-hexane (**9**).* Compound (**9**) was obtained by heating solution of 1,6-bis-[8-(propyltosylamino)phenanthridine-6-yl]-hexane **3** (27 mg, 0.032 mmol) in a mixture of concd H_2SO_4 (1 ml) and concd acetic acid (2 ml) under reflux at 80–100 °C for 2 h. The reaction mixture was cooled, poured on ice, and made alkaline (pH=8–9) by addition of 2 M NaOH. The obtained yellow-brown solid was precipitated, filtered, and washed with lots of water to afford pure compound **9** (5 mg, 28% yield); mp 221–224 °C; R_f (SiO_2, 10% MeOH in CH_2Cl_2)=0.49; ^{1}H NMR (DMSO-d_6) δ: 0.94 (t, CH_3, 6H, J=7.5 Hz), 1.57–1.64 (m, CH_2–hexylene, CH_2–propyl chain, 8H), 1.89 (br s, CH_2–hexylene, 4H), 3.12 (br s, CH_2–hexylene, 4H), 6.28 (br s, NH, 2H), 7.12 (s, Phen-7, 2H), 7.27 (d, Phen-9, 2H, J_{9-10}=7.8 Hz), 7.46–7.53 (m, Phen-2, Phen-3, 4H), 7.88 (m, Phen-4, 2H), 8.49 (m, Phen-1, Phen-10, 4H) ppm; IR (KBr) ν: 3447, 3246, 2961, 2926, 2854, 2361, 2334, 1653, 1618, 1541, 1508, 1458, 1387, 1340, 1315, 1256, 1232, 1205, 1140, 824, 762, 669, 598, 517 cm^{-1}; (MALDI/TOF-HRMS) m/z: 555.3493 (calcd for $C_{38}H_{42}N_4$: 555.3482).

*4.4.10. 1-[8-(3-(Urac-1-il)propyl)aminophenanthridine-6-yl]-6-[8-(propyl) aminophenanthridine-6-yl]hexane (**10**).* Compound (**10**) was obtained as described for **9**; 1-[8-(3-(urac-1-il)propyltosyl)aminophenanthridine-6-yl]-6-[8-(propyltosyl)aminophenanthridine-6-yl]hexane **6** (40 mg, 0.04 mmol) in concd H_2SO_4 (1 ml) gave yellow powder **10** (15 mg, 53% yield); mp 108–110 °C; R_f (SiO_2, 10% MeOH in CH_2Cl_2)=0.39; ^{1}H NMR (DMSO-d_6) δ: 0.94 (t, CH_3, 3H, J=7.4 Hz), 1.59 (m, CH_2–hexylene chain, CH_2–propyl chain, 6H), 1.90 (m, CH_2–hexylene chain, CH_2–propylene chain, 6H), 3.12 (m, NCH_2, 2H), 3.,21 (m, CH_2–hexylene chain, 4H), 3.79 (t, uracil-NCH_2–propylene chain, 2H, J=6.3 Hz), 5.54 (d, uracil-5, 1H, J_{5-6}=7.9 Hz), 6.27 (NH, br s, 2H), 7.14 (dd, Phen-9, 2H,), 7.25 (s, Phen-7, 1H), 7.28 (s, Phen-7, 1H),7.50 (m, Phen-2, Phen-3, 4H), 7.62 (d, uracil-6, 1H), 7.87 (d, Phen-4, 2H), 8.51 (m, Phen-1, Phen-10), 11.25 (s, uracil-NH, 1H) ppm; ^{13}C NMR (DMSO-d_6) δ: 11.23 (CH_3), 21.81 (CH_2–propyl chain), 27.41 (CH_2–propylene chain), 29.21 (Phen-CH_2), 29.76 (Phen-CH_2), 36.05 (Phen-CH_2), 46.51 (uracil-NCH_2–propylene chain). 47.69 ($NHCH_2$–propylene chain), 52.35 ($NHCH_2$–propyl chain), 102.27 (uracil-5); IR (KBr) ν: 3398, 3057, 2926, 2853, 2363, 2345, 1684, 1655, 1618, 1541, 1508, 1458, 1387, 1340, 1259, 1232, 1200, 1136, 1034, 997, 949, 864, 824, 760, 721, 669, 617, 548 cm^{-1}; (MALDI/TOF-HRMS) m/z: 665.3580 (calcd for $C_{42}H_{44}N_6O_2$: 665.3599).

*4.4.11. 1-[8-(9-(Aden-1-yl)propyl)aminophenanthridine-6-yl]-6-[8-(propyl)aminophenanthridine-6-yl]hexane (**11**).* Compound (**11**) was obtained as described for **9**; 1-[8-(9-(aden-1-yl)propyltosyl)-aminophenanthridine-6-yl]-6-[8-(propyltosyl)aminophenanthridine-6-yl]hexane **7** (45 mg, 0.045 mmol) in concd H_2SO_4 (1 ml) and concd acetic acid (2 ml) gave yellow powder **11** (15 mg, 50% yield); R_f (SiO_2, 10% MeOH in CH_2Cl_2)=0.32; mp 119–122 °C; ^{1}H NMR (DMSO-d_6) δ: 0.90 (t, CH_3, 3H, J=7.4 Hz), 1.51–1.61 (m, CH_2–hexylene chain, CH_2–propyl chain, 6H), 1.88 (br s, Phen-CH_2, 4H), 2.13 (m, CH_2–propylene chain, 2H), 3.08 (m, $NHCH_2$–propyl chain, 2H), 3.16–3.21(m, Phen-CH_2, $NHCH_2$–propylene chain, 6H), 4.27 (t, adenine–NCH_2–propylene chain, 2H, J=6.7 Hz), 6.26 (br s, NH, 1H), 6.39 (br s, NH, 1H), 7.10 (s, Phen-7, 2H), 7.21–7.29 (m, adenine–NH_2, Phen-9, Phen-7, 5H), 7.48–7.52 (m, Phen-2, Phen-3, 4H), 7.86 (m, Phen-4, H), 8.14 (br s, adenine-2, adenine-8, 2H), 8.46–8.52 (m, Phen-1, Phen-10, 4H) ppm; ^{13}C NMR (DMSO-d_6) δ: 11.80 (CH_3), 21.83, 28.07, 28.21, 28.92, 29.19, 29.29, 41.21, 44.70, 103.02, 103.32, 114.63, 119.04, 119.65, 120.59, 121.29, 121.36, 122.63, 122.93, 123.74, 123.86, 124.14, 124.22, 126.20. 126.24, 126.31, 126.73, 126.75, 129.05, 129.08, 129.62, 141.50, 141.58, 148.36. 148.70, 149.79, 152.55, 156.15, 160.59, 160.70 ppm; IR (KBr) ν: 3447, 2928, 2853, 2361, 2343, 1869, 1772, 1734, 1647, 1618, 1541, 1508, 1458, 1387, 1339, 1315, 1259, 1232, 1200, 822, 760, 669, 650, 519 cm^{-1}; (MALDI/TOF-HRMS) m/z: 688.3886 (calcd for $C_{43}H_{45}N_9$: 688.3871).

*4.4.12. 1,6-Bis-[8-(3-(aden-9-yl)propylamino)phenanthridine-6-yl]-hexane (**12**).* Compound (**12**) was obtained as described for **9**; 1,6-bis-[8-(3-(aden-9-yl)propyltosylamino)phenanthridine-6-yl]-hexane **8** (30 mg, 0.027 mmol) in concd H_2SO_4 (1 ml) and concd acetic acid (2 ml) gave yellow powder **12** (17 mg, 77% yield); R_f (SiO_2, 10% MeOH in CH_2Cl_2)=0.45 mp 147–149 °C; ^{1}H NMR (DMSO-d_6) δ: 11.53 (br s, CH_2–hexylene chain, 4H), 1.85 (br s, CH_2–hexylene chain, 4H); 2.26 (m, CH_2–propylene chain, 4H), 3.15 (m, CH_2–hexylene chain, NCH_2, 8H), 4.26 (t, adenine–NCH_2–propylene chain, 4H, J=6.7 Hz), 6.38 (br s, NH, 2H), 6.98 (s, Phen-7, 2H), 7.22 (m, adenine–NH_2, Phen-9, 6H), 7.48–7.51 (m, Phen-2, Phen-3, 4H), 7.86 (m, Phen-4, H), 8.12 (s, adenine, 2H), 8.13 (s, adenine, 2H), 8.44–8.51 (m, Phen-1, Phen-10, 4H) ppm; ^{13}C NMR (DMSO-d_6) δ: 27.91, 28.7, 29.08, 35.11, 38.28, 41.01, 119.44, 121.33, 123.71, 123.95, 126.1, 126.53, 128.92, 130.79, 133.99, 138.37, 141.14, 141.4, 142.18, 148.18, 149.57, 155.99, 158.99, 160.45 ppm; IR (KBr) ν: 3337, 3200, 2924, 2852, 1640, 1619, 1575, 1541, 1479, 1462, 1420, 1395, 1335, 1308, 1240, 1210, 1178, 830, 800, 762, 730, 660 cm^{-1}; (MALDI/TOF-HRMS) m/z: 821.4279 (calcd for $C_{48}H_{48}N_{14}$: 821.4259).

Acknowledgements

We thank the Ministry of Science, Education and Sport of the Republic of Croatia for financial support of this study (grants no. 098-0982914-2918 and 098-1191344-2860).

Supplementary data

The UV–vis spectra of studied nucleotides, additional molecular modeling results associated with this article can be found in online version at doi:10.1016/j.tet.2010.01.063.

References and notes

1. (a) Lehn, J. M. *Supramolecular Chemistry. Concepts and Perspectives*; Wiley-VCH: Weinheim, 1995; (b) Atwood, J. L. *Comprehensive and Supramolecular Chemistry*; Pergamon: Oxford, 1996.
2. (a) De Silva, A. P.; Gunaratne, H. Q. N.; Gunnlaugsson, T.; Huxley, A. J. M.; McCoy, C. P.; Rademacher, J. T.; Rice, T. E. *Chem. Rev.* **1997**, *97*, 1515; (b) Sessler, J. L.; Kral, V.; Shishkanova, T. V.; Gale, P. A. *Proc. Natl. Acad. Sci. U.S.A.* **2002**, *99*, 4848.
3. Constant, J.-F.; Fahy, J.; Lhomme, J. *Tetrahedron Lett.* **1987**, *28*, 1777.
4. Shionoya, M.; Ikeda, T.; Kimura, E.; Shiro, M. *J Am Chem Soc.* **1994**, *116*, 3848.
5. Aoki, S.; Kimura, E. *J. Am. Chem. Soc.* **2000**, *122*, 4542.
6. (a) Teulade-Fichou, M.-P.; Vigneron, J.-P.; Lehn, J.-M. *Supramol. Chem.* **1995**, *5*, 139; (b) Baudoin, O.; Gonnet, F.; Teulade-Fichou, M.-P.; Vigneron, J.-P.; Tabet, J.-C.; Lehn, J.-M. *Chem.—Eur. J* **1999**, *5*, 2762.
7. Piantanida, I.; Palm, B. S.; Čudić, P.; Žinić, M.; Schneider, H.-J. *Tetrahedron Lett.* **2001**, *42*, 6779.
8. Čudić, P.; Žinić, M.; Tomišić, V.; Simeon, V.; Vigneron, J.-P.; Lehn, J.-M. *J. Chem. Soc., Chem. Commun.* **1995**, 1073.
9. Meyer, E. A.; Castellano, R. K.; Diederich, F. *Angew. Chem., Int. Ed* **2003**, *42*, 1210.
10. Schneider, H.-J.; Yatsimirsky, A. In *Principles and Methods in Supramolecular Chemistry*; Wiley-VCH: Weinheim, 2000.
11. Tumir, L.-M.; Piantanida, I.; Novak, P.; Žinić, M. *J. Phys. Org. Chem.* **2002**, *15*, 599.
12. Tumir, L.-M.; Piantanida, I.; Juranović Cindrić, I.; Hrenar, T.; Meić, Z.; Žinić, M. *J. Phys. Org. Chem.* **2003**, *16*, 891.
13. Tumir, L.-M.; Piantanida, I.; Žinić, M.; Juranović Cindrić, I.; Meić, Z.; Kralj, M.; Tomić, S. *Eur. J. Med. Chem.* **2006**, *41*, 1153.
14. Juranović, I.; Meić, Z.; Piantanida, I.; Tumir, L.-M.; Žinić, M. *Chem. Commun.* **2002**, 1432.
15. Tumir, L.-M.; Piantanida, I.; Juranović, I.; Meić, Z.; Tomić, S.; Žinić, M. *Chem. Commun.* **2005**, 2561.
16. Čudić, P.; Žinić, M.; Škarić, V.; Kiralj, R.; Kojić-Prodić, B.; Vigneron, J.-P.; Lehn, J.-M. *Croat. Chem. Acta* **1996**, *69*, 569.
17. Morgan, G. T.; Walls, L. P. *J. Chem. Soc.* **1931**, 2447.
18. Jones, R. L.; Wilson, W. D. *Biopolymers* **1981**, *20*, 141.
19. Specfit Global Analysis Program Gampp, H.; Maeder, M.; Meyer, C. J.; Zuberbuehler, A. D. *Talanta* **1985**, *32*, 257; Maeder, M.; Zuberbuehler, A. D. *Anal. Chem.* **1990**, *62*, 2220.
20. Wakelin, L. P. G. *Med. Res. Rev.* **1986**, *6*, 275.
21. Demeunynck, M.; Bailly, C.; Wilson, W. D. In *DNA and RNA binders*; Wiley-VCH: Weinheim, 2002.
22. Čudić, P.; Žinić, M.; Tomišić, V.; Simeon, V.; Vigneron, J.-P.; Lehn, J.-M. *J. Chem. Soc., Chem. Commun.* **1995**, 1073.
23. INSIGHTII. *Accelerys*; 2001–2008; http://accelrys.com/services/training/life-science/insight-migration.html San Diego.
24. Duan, Y.; Wu, C.; Chowdhury, S.; Lee, M. C.; Xiong, G.; Zhang, W.; Yang, R.; Cipelak, P.; Luo, R.; Lee, T. *J. Comput. Chem.* **2003**, *24*, 1999.
25. http://amber.scripps.edu/.